

Thermodynamic superheating and relevant interface stability of low-dimensional metallic crystals

This article has been downloaded from IOPscience. Please scroll down to see the full text article.

2001 J. Phys.: Condens. Matter 13 565

(<http://iopscience.iop.org/0953-8984/13/4/303>)

View [the table of contents for this issue](#), or go to the [journal homepage](#) for more

Download details:

IP Address: 171.66.16.226

The article was downloaded on 16/05/2010 at 08:21

Please note that [terms and conditions apply](#).

Thermodynamic superheating and relevant interface stability of low-dimensional metallic crystals

Q Jiang¹, L H Liang and J C Li

Department of Materials Science and Engineering, Jilin University of Technology,
Changchun 130025, People's Republic of China

E-mail: jiangq@post.jut.edu.cn

Received 7 November 2000

Abstract

In terms of a model for size-dependent melting and the Lindemann criterion, a model to interpret thermodynamic superheating of all low-dimensional metallic crystals is developed. A superheating is present when the metallic nanocrystals have coherent or semi-coherent interfaces with the surrounding matrix and when the atomic diameter of the nanocrystals is larger than that of the matrix. The superheating temperatures of the nanocrystals are lower than the stability temperatures of the coherent interfaces. The model prediction shows good agreement with the experimental evidence.

1. Introduction

The melting points of low-dimensional crystals in freestanding states, such as nanoparticles, nanowires and thin films, are considerably reduced relative to the melting points of the corresponding bulk crystals [1–2]. While more and more applications have been found for low-dimensional materials in modern industries [3], their stability against melting is becoming one of the major concerns in further development and applications of this new family of materials [4–15]. Although thermodynamic superheating of nanoparticles embedded in a matrix with a higher melting temperature has been expected and found in many systems [4–14], thin films sandwiched within thicker layers have recently been reported to be thermodynamically superheated [15]. A body of experimental evidence indicates that the necessary condition of this superheating is the existence of coherent interfaces between the nanoparticles and the surrounding matrix [7–13, 15]. Under this condition, the superheating has been interpreted through various pressure effects [10], such as a capillary effect due to the decreasing size, the different thermal expansion between the matrix and the nanocrystals and the effect due to volume change during melting. However, the above considerations become less important for superheating of films since the films are infinite in two dimensions and thus have no curvature-induced pressure effect. In addition, many analyses imply that the superheating of nanocrystals is a kinetic superheating due to blocking surface melting [16] or a difficulty in the nucleation of liquid [10, 15], which

¹ Author to whom correspondence should be addressed.

is not consistent with the experimental fact that these low-dimensional crystals can exist in a superheating state for hours. Moreover, the thermodynamic stability condition of the interfaces has not been considered, which controls the possibility of superheating. Thus, quantitative estimates matching with the observed thermodynamic superheating are lacking [10].

Recently, a model on the basis of the Lindemann criterion for melting and Mott's expression for the vibrational entropy of melting has predicted the size-dependent melting depression for all low-dimensional nanocrystals, including thin films [1–2, 13], and has been confirmed by available experimental evidence. Moreover, the model prediction for superheating of nanoparticles embedded in a matrix with coherent interfaces also shows that it is applicable [13]. Note that although superheating usually means heating above the thermodynamic transition temperature (the melting point) to a region where the phase is metastable, the concept of superheating here is a thermodynamic melting correlated with the Lindemann criterion [17].

In this paper, the model is extended to interpret the superheating behaviour of all low-dimensional metallic nanocrystals. According to the model, when interfaces between the confined nanocrystals and the surrounding matrix are coherent or semi-coherent and when the atomic diameter of the surrounding matrix is smaller than that of the nanocrystals, the thermal vibration of atoms of the nanocrystals at the interface is suppressed. This suppression leads to not only an absence of surface melting, but also to thermodynamic superheating.

2. Model

The size dependence of the melting point $T_m(D)$ of low-dimensional nanocrystals (in the following low-dimensional nanocrystals are uniformly called as nanocrystals) with a diameter D is given by [1, 2]

$$T_m(D)/T_m(\infty) = \sigma_m^2(\infty)/\sigma_m^2(D) = \exp[(1 - \alpha)/(D/D_0 - 1)] \quad (1)$$

where $\sigma_m^2(D)$ is the averaged mean-square displacement (msd) of atoms of the nanocrystals at $T_m(D)$, $T_m(\infty)$ and $\sigma_m^2(\infty)$ are the corresponding bulk values for $T_m(D)$ and $\sigma_m^2(D)$, respectively. For a nanoparticle, D has the usual meaning of diameter. For a nanowire, D is taken as its diameter. For a film, D denotes its thickness. D_0 denotes a critical diameter at which almost all atoms of the nanocrystal are located on the surface. The value of D_0 depends on the dimension of the crystal d where $d = 0$ for nanoparticles, $d = 1$ for nanowires and $d = 2$ for films. The relationship between D_0 and d is [1–2]

$$D_0 = 2(3 - d)h \quad (2)$$

with h being the atomic diameter. α in equation (1) is the ratio between the msd of atoms on the surface ($\sigma_{ms}^2(D)$) and that of those inside the nanocrystals ($\sigma_{mv}^2(D)$) [1–2, 18], i.e. $\alpha = \sigma_{ms}^2(D)/\sigma_{mv}^2(D)$ where $\sigma_{mv}^2(D) \approx \sigma_m^2(\infty)$ [18]. For the nanocrystals confined in a matrix or thicker layers with coherent interfaces, it is expected that the msd value of the surface atoms of the nanocrystals falls between that of the interior atoms of the nanocrystals and that of the atoms of the matrix. Thus, α could simply be estimated as a mean value between them [13]:

$$\alpha = \{[\sigma_m^2(\infty) + \sigma_M^2(T_m(D))]/2\}/\sigma_m^2(\infty) = [\sigma_M^2(T_m(D))/\sigma_m^2(\infty) + 1]/2 \quad (3)$$

where $\sigma_M^2(T_m(D))$ is the averaged msd value of the atoms of the matrix at $T_m(D)$. Note that σ_M^2 is specially displayed here as the function of the specific temperature and different from the other simplified expression.

According to the Lindemann criterion [17, 18], a crystal melts when the root msd of the atoms of the crystal exceeds a certain fraction of h , or

$$\sigma/h = c \quad (4)$$

where c is a constant, although c slightly varies with crystal structure. It is 0.13 for fcc crystals and 0.18 for bcc crystals [19]. This difference is partly induced by the change of h , which depends on the coordination number of the lattice [20]. A smaller coordination number corresponds to a larger h [20]. In order to reduce or eliminate this difference among distinct lattices or coordination numbers, h here is calculated by the atomic volume, which is little dependent on the lattice structure [20]. With h so defined, c is almost lattice independent. Thus, $\sigma_M(\infty)/h_M = \sigma_m(\infty)/h_N$ where $\sigma_M(\infty)$ denotes the root msd of the atoms of the matrix at the corresponding bulk melting temperature $T_M(\infty)$ and h_M and h_N show the atomic diameters of the matrix and nanocrystals, respectively.

Since $T_m(D)$ is usually higher than the bulk Debye temperature of the matrix [1, 2], the high-temperature approximation for $\sigma_M^2(T)$ at a temperature T can be utilized [17, 18]:

$$\sigma_M^2(T) = kT/[m(2\pi\nu_E)^2] \quad (5)$$

where m is the atomic mass, ν_E is the Einstein frequency and k is Boltzmann's constant. Substituting $T = T_M(\infty)$ and $T = T_m(D)$ into (5), their ratio is as follows:

$$\sigma_M^2(T_m(D))/\sigma_M^2(\infty) = T_m(D)/T_M(\infty). \quad (6)$$

Substituting $\sigma_M^2(\infty) = [h_M/h_N]^2\sigma_m^2(\infty)$ in terms of (4) into (6), $\sigma_M^2(T_m(D))/\sigma_M^2(\infty) = [h_M/h_N]^2[T_m(D)/T_M(\infty)]$. Thus, $\alpha = [(h_M/h_N)^2T_m(D)/T_M(\infty) + 1]/2$ according to (3). Since the difference between $T_m(D)/T_M(\infty)$ and $T_m(\infty)/T_M(\infty)$ is small (see figures 1–4 below, even if D is as small as 10 nm, $[T_m(D) - T_m(\infty)]$ is only several tens of kelvin, while $T_M(\infty)$ is at least several hundred kelvin), α is a weak function of D . As a first-order approximation $T_m(\infty)$ takes the place of $T_m(D)$ or α takes its smallest value. Finally, we have

$$\alpha = [(h_M/h_N)^2T_m(\infty)/T_M(\infty) + 1]/2. \quad (7)$$

Substituting (7) into (1), the size-dependent superheating can be predicted. The necessary parameters used in the equations are only concerned with the well known atomic diameters and bulk melting temperatures of the nanocrystals and the matrix.

Note that the validity of (1) depends on the stability of the interfaces between the matrix and the nanocrystals. When a liquid layer on the interface is formed, which results in the replacement of a nanocrystal–matrix interface by two solid–liquid interfaces, melting of the total nanocrystals occurs at once. Thus, the stability of the interface is controlled by the interface energy change $\Delta\gamma$ during the above transition. Only when $\Delta\gamma > 0$ can superheating of nanocrystals exist. We assume the liquid layer on the interface only consists of the component of nanocrystals, since the temperature is lower than the melting temperature of the matrix and the mutual solubility in any superheating system is negligibly small [10]. Let γ_{sl} and γ_{GB} be the solid–liquid interface energy and solid–solid interface energy for the same material, in the following superscripts M and N denote matrix and nanocrystals, respectively. The γ_{sl} deduced from the Gibbs–Thomson equation is determined by [21]

$$\gamma_{sl} = 2hS_mH_m/(3RV_g) \quad (8)$$

where V_g is the molar volume, S_m and H_m show the melting entropy and enthalpy of bulk crystals and R denotes the ideal gas constant. Note that [22]

$$\gamma_{GB} \approx 2\gamma_{sl} \quad (9)$$

which is in agreement with the phenomenological equation $\gamma_{GB} \approx 1.3hH_m/V_g$ [23] if $S_m/R \approx 1$ and $1.3 \approx 4/3$. When a liquid layer is formed,

$$\Delta\gamma = \gamma_{sl}^{MN} + \gamma_{sl}^N - \gamma_{GB}^{MN} \quad (10)$$

where the liquid–matrix interface energy γ_{sl}^{MN} is assumed to be $(\gamma_{sl}^M + \gamma_{sl}^N)/2$, the liquid–nanocrystal interface energy γ_{sl}^N is calculated by (8), the nanocrystal–matrix interface

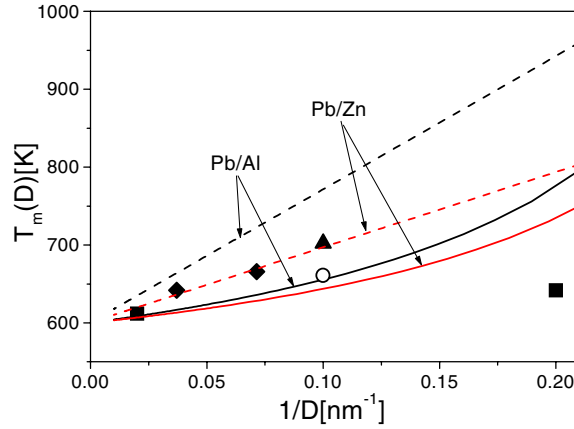


Figure 1. $T_m(D)$ (full curves) and $T_{max}(D)$ (broken curves) functions for the Pb/Al and Pb/Zn systems in terms of equations (1) and (12). For the Pb/Al system, $h_M = 0.3164$ nm [20], $h_N = 0.3898$ nm [20], $D_0 = 6h_N = 2.3388$ nm in terms of (2), $T_M(\infty) = 933.25$ K, $T_m(\infty) = 600.6$ K [27], $\alpha = 0.71$ in terms of (7), $V_g^N = 18.17$ cm³ mol⁻¹, $V_g^M = 10$ cm³ mol⁻¹ [27], $H_m^N(\infty) = 4799$ J mol⁻¹ and $H_m^M(\infty) = 10790$ J mol⁻¹ [27]; the experimental results are shown as \blacklozenge [6], \blacktriangle [9] and \blacksquare [10]. For the Pb/Zn system, $h_M = 0.3076$ nm [20], $T_M(\infty) = 692.73$ K [27], $\alpha = 0.77$ in terms of (7), $V_g^M = 9.2$ cm³ mol⁻¹ and $H_m^M(\infty) = 7322$ J mol⁻¹ [27]; \circ denotes the experimental data [8].

energy γ_{GB}^{MN} is roughly estimated to be γ_{GB}^N . The reason for this consideration is that the nanocrystals having coherent interfaces with the matrix can be indeed superheated experimentally, $\Delta\gamma$ must be positive [24]. Three approximate values of calculable interface energy for γ_{GB}^{MN} in terms of (8) and (9), are γ_{GB}^M , $(\gamma_{GB}^M + \gamma_{GB}^N)/2$ and γ_{GB}^N respectively. Only when $\gamma_{GB}^{MN} = \gamma_{GB}^N$, $\Delta\gamma > 0$. In terms of equations (8) and (9), we have

$$\Delta\gamma = [h_M S_m^M H_m^M / V_g^M - h_N S_m^N H_m^N / V_g^N] / (3R). \quad (11)$$

Up to the point where $\Delta\gamma$ is balanced with the volume Gibbs free energy of the nanocrystals $\mu = S_m^N [T_{max}(D) - T_m(\infty)]$, where $T_{max}(D)$ is the size-dependent maximal superheating temperature, or $(h_N D / D_0) S_m^N [T - T_m(\infty)] / V_g^N = \Delta\gamma$, with $h_N D / D_0$ suiting different dimensions, the interface remains stable. In terms of (11), we obtain

$$T_{max}(D) / T_m(\infty) = 1 + D_0 [(h_M / h_N) (H_m^M / H_m^N) (V_g^N / V_g^M) S_m^M - S_m^N] / (3RD). \quad (12)$$

Note that $T_{max}(D) < T_m(D)$ only occurs as $D \rightarrow D_0$. Thus, the instability of coherent interfaces does not change the validity of (1), at least for relatively large particles.

3. Results and discussion

To confirm our model, experimental results of superheating, are summarized in figures 1–3 (nanoparticles) and 4 (thin films). The experimental results of the Pb/Al system (referring to Pb nanoparticles embedded in an Al matrix, the following expressions have a similar meaning) [6, 9–10] and the Pb/Zn system [8] are plotted in figure 1, the In/Al system [5, 7, 11–12] in figure 2, the Ag/Ni system [14] in figure 3 and Pb/Al films system (Pb thin films sandwiched within Al layers) in figure 4 [15]. It is obvious that the predictions for different systems with distinct dimensions show good agreement with the experimental data of different authors. In addition, all the stability temperatures of the interfaces are higher than the thermodynamic melting temperatures in the measured size range. Since the superheating of thin films in

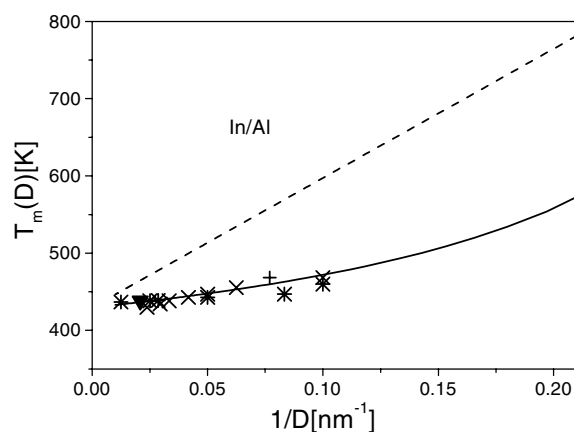


Figure 2. $T_m(D)$ (full curves) and $T_{max}(D)$ (broken curves) functions for the In/Al system in terms of equations (1) and (12). $h_N = 0.3682$ nm [20], $D_0 = 6h_N = 2.2092$ nm, $T_m(\infty) = 429.76$ K [27], $\alpha = 0.67$ in terms of (7), $V_g^N = 15.7$ cm³ mol⁻¹ and $H_m^N(\infty) = 3263$ J mol⁻¹ [27]. The experimental evidence is shown as \times [5], $+$ [7], ∇ [11] and $*$ [12].

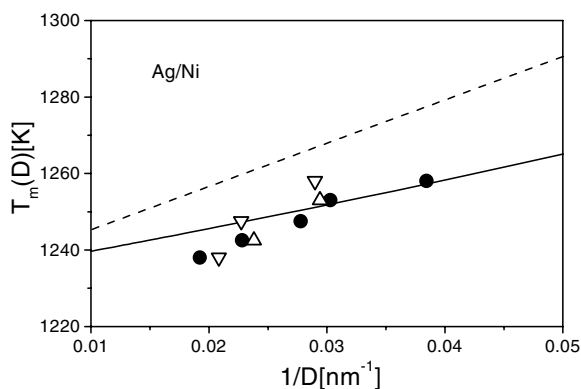


Figure 3. $T_m(D)$ (full curve) and $T_{max}(D)$ (broken curve) functions for the Ag/Ni system in terms of equations (1) and (12). $h_M = 0.2754$ nm [20], $h_N = 0.3196$ nm [20] with $D_0 = 6h_N = 1.9176$ nm in terms of (2), $T_M(\infty) = 1726$ K, $T_m(\infty) = 1234$ K [27], $V_g^N = 10.3$ cm³ mol⁻¹ and $V_g^M = 6.59$ cm³ mol⁻¹ [27], $H_m^N(\infty) = 11300$ J mol⁻¹ and $H_m^M(\infty) = 17470$ J mol⁻¹ [27]. $\alpha = 0.77$ in terms of (7). The experimental results are plotted as \bullet , Δ and ∇ (each referring to a different sample) [14].

figure 4 corresponds well to our prediction, our model can indeed describe the superheating behaviours of all low-dimensional crystals.

As shown in (1) and figures 1–4, $T_m(D)$ depends on D and α . Only when $\alpha < 1$ do $T_m(D)/T_m(\infty) > 1$ and $T_m(D)$ increase as D decreases. $\alpha < 1$ implies that the effect of the compressive force is essentially on the surface atoms of nanocrystals. As D decreases, the percentage of the surface atoms of the nanocrystals increases and the effect of the compressive force is enhanced. In the realistic systems in figures 1–4, α is in the range of 0.67–0.77, which gives an upper thermodynamic superheating of $T_m(2D_0)$ between $1.39T_m(\infty)$ and $1.26T_m(\infty)$ if we assume that the smallest nanocrystal has a diameter of $2D_0$. The corresponding interface stability temperatures are $1.24T_m(\infty)$ for the Ag/Ni system, $1.61T_m(\infty)$ for the Pb/Al system,

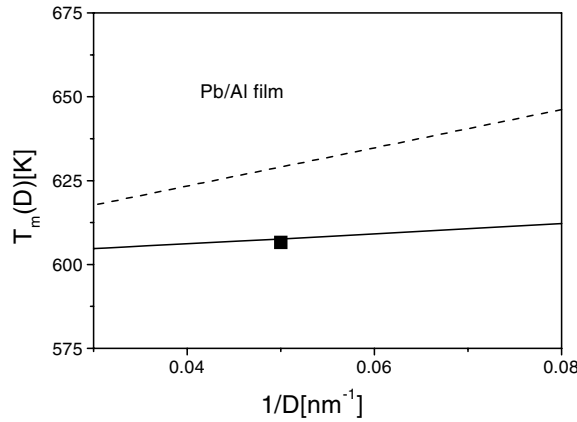


Figure 4. $T_m(D)$ (full curve) and $T_{max}(D)$ (broken curve) functions for the Pb/Al film system plotted by equations (1) and (12). The parameters used in the figure are given in the caption of figure 1; however, $D_0 = 2h_N = 0.7796$ nm in terms of (2). The experimental results are shown as ■ [15].

$1.88T_m(\infty)$ for the In/Al system and $1.34T_m(\infty)$ for the Pb/Zn system. Only for the Ag/Ni system is $T_{max}(2D_0) < T_m(2D_0)$, due to a smaller difference of $S_m(\infty)$ between the Ag and the Ni than the elements in the other systems. Note that the kinetic superheating limits calculated by the entropy catastrophe of bulk crystals [25] and by the homogeneous nucleation theory of surface free bulk crystals [26] are about $1.2T_m(\infty)$. The nanocrystals confined in a matrix can thermodynamically exist above this temperature as long as the diameter of the nanocrystals is small enough. When $D < 2D_0$, stronger superheating, such as an Ar bubble in an Al matrix, can be observed, although now the Ar bubbles of this size are possibly no longer independent crystals in the matrix [4].

According to (7), $\alpha < 1$ is obtained by $T_m(\infty)/T_M(\infty) < h_N^2/h_M^2$, while $T_m(\infty)/T_M(\infty) < 1$ is necessary and understandable for superheating; also $h_N/h_M > 1$ in all reported systems (see the captions of figures 1–4). It is plausible that if $h_N/h_M < 1$, the local interface stress for the nanocrystals on the coherent interface is tensile [27], which locally increases, but does not decrease, the msd of the surface atoms of the nanocrystals. Thus, $h_N/h_M > 1$ should be a sufficient condition for superheating and has also a contribution in the decreasing of α . The above consideration is especially true since the components of a system are chosen to prevent compound formation and to minimize mutual solubility, both of these will create stress effects [28]. However, the condition of $h_N/h_M > 1$ for superheating is valid only when the atomic distances of both components on the interface are equal to or equally proportional to their atomic diameters. Otherwise, if the atomic distance of the matrix on a semi-coherent interface is larger than the corresponding atomic distance of the nanocrystal, such as the Pb/Ni system (even if $h_N/h_M > 1$) with an orientation relationship of $(100)_{Pb}/(100)_{Ni}$ and $[001]_{Pb}/[011]_{Ni}$, superheating is still absent where the two atomic distance of Ni along the $[011]$ direction is larger than one atomic distance of Pb along the $[001]$ direction [10].

The above experimental results and theoretical predictions differ from the results of kinetic superheating, such as bulk Ag (in the order of micrometres) coated by Au [29]. In this case, the coating layer of Au hinders the surface melting of Ag and yields kinetic superheating [29]. However, as indicated by (1), the percentage of surface atoms from the total atoms of the bulk crystal is negligible. Thus, the averaged msd of the atoms of the crystal and its melting point still hold the bulk values.

4. Conclusions

In summary, a simple model based on the suppression of thermal vibrations of atoms on the surface of nanocrystals is developed to account for size-dependent superheating of both metallic nanoparticles and thin films confined in a matrix. According to the model, superheating of nanocrystals occurs when the melting temperature of the matrix is higher than that of nanocrystals, the interfaces between the nanocrystals and the matrix are coherent or semi-coherent and produce a compressive stress on the nanocrystals. The superheating of nanocrystals is not disturbed by the instability of the interfaces. Experimental evidence confirms the present model.

Acknowledgments

The financial support of the National Natural Science Foundation of China under grant No 59931030 and the Trans-Century Training Program Foundation for the Talents by the Ministry of Education of China are acknowledged.

References

- [1] Jiang Q, Shi H X and Zhao M 1999 *J. Chem. Phys.* **111** 2176
- [2] Jiang Q, Tong H Y, Hsu D T, Okuyama K and Shi F G 1998 *Thin Solid Films* **312** 357
- [3] Gleiter H 2000 *Acta Mater.* **48** 1
- [4] Rossouw C J and Donnelly S E 1985 *Phys. Rev. Lett.* **55** 2960
- [5] Saka H, Nishikawa Y and Imura T 1988 *Phil. Mag. A* **57** 895
- [6] Gråback L and Bohr J 1990 *Phys. Rev. Lett.* **64** 934
- [7] Zhang D L and Cantor B 1991 *Acta Metall. Mater.* **39** 1595
- [8] Goswami R and Chattopadhyay K 1993 *Phil. Mag. Lett.* **68** 215
- [9] Sheng H W, Ren G, Peng L M, Hu Z Q and Lu K 1996 *Phil. Mag. Lett.* **73** 179
- [10] Chattopadhyay K and Goswami R 1997 *Prog. Mater. Sci.* **42** 287
- [11] Sheng H W, Ren G, Peng L M, Hu Z Q and Lu K 1997 *J. Mater. Res.* **12** 119
- [12] Lu K, Sheng H W and Jin Z H 1997 *Chinese J. Mater. Res.* **11** 658 (in Chinese)
- [13] Jiang Q, Zhang Z and Li J C 2000 *Chem. Phys. Lett.* **322** 549
- [14] Zhong J, Zhang L H, Jin Z H, Sui M L and Lu K 2000 *Acta Mater.* submitted
- [15] Zhang L, Jin Z H, Zhang L H, Sui M L and Lu K 2000 *Phys. Rev. Lett.* **85** 1484
- [16] Cahn R W 1986 *Nature* **323** 668
- [17] Dash J G 1999 *Rev. Mod. Phys.* **71** 1737
- [18] Shi F G 1994 *J. Mater. Res.* **9** 1307
- [19] Stillinger F H 1995 *Science* **267** 1935
- [20] King H K 1970 *Physical Metallurgy* ed R W Cahn (Amsterdam: North-Holland) pp 59–63
- [21] Jiang Q, Shi H X and Zhao M 1999 *Acta Mater.* **47** 2109
- [22] Kotze I A and Kuhlmann-Wilsdorf D 1966 *Appl. Phys. Lett.* **9** 96
- [23] Weissmüller J 1993 *Nanostruct. Mater.* **3** 261
- [24] Goswami R, Chattopadhyay K and Ryder P L 1998 *Acta Mater.* **46** 4257
- [25] Fecht H J and Johnson W L 1988 *Nature* **334** 50
- [26] Lu K and Li Y 1998 *Phys. Rev. Lett.* **80** 4474
- [27] Sargent-Welch Scientific Company 1979 *Periodic Table of the Elements* (Skokie, Sargent-Welch) p 1
- [28] Spaepen F 2000 *Acta Mater.* **48** 31
- [29] Dâges J, Gleiter H and Perepezko J H 1986 *Phys. Lett. A* **119** 79